Photoelectrochemistry and Etching of SiC: a Comparison with Si

J J Kelly[1], D H van Dorp[1], J L Weyher[2]

1) Condensed Matter and Interfaces, Debye Institute, Utrecht University, Princetonplein 1, 3508 TA Utrecht, The Netherlands
2) Applied Materials Science, Institute for Molecules and Materials, Radboud University Nijmegen, Toernooiveld 1, 6526 ED Nijmegen, The Netherlands

Abstract

The anodic electrochemistry and etching of the group IV compound semiconductor SiC was studied in both KOH and acidic fluoride solutions. The results for p-type and n-type electrodes are compared with those obtained for the group IV elemental semiconductor Si. We point out a number of interesting applications of this work for SiC device technology.

Introduction

Silicon has a very rich chemistry in aqueous solution. At high pH the semiconductor etches chemically [1]. Since this reaction is highly anisotropic, etching reveals crystallographic planes at resist edges. The resulting forms are widely used in micro-electromechanical systems (MEMS) [2, 3]. Silicon can also be anodically oxidized in alkaline solution and passivated at positive potential [4]. These reactions are observed, not only for the p-type electrode but, surprisingly at comparable current density, also for n-type Si. A combined chemical-electrochemical mechanism has been proposed to explain these results [5]. The anodic passivation of n-type silicon forms the basis for an etch-stop mechanism important for membrane fabrication in MEMS [6, 7]. At low pH, fluoride in solution is required to prevent passivation of Si. In this case the "normal" semiconductor electrochemistry is observed: the p-type electrode can be anodically oxidized in the dark; supra bandgap light is required to oxidize the n-type electrode. In the onset of the anodic (photo)current-potential curve, porous silicon is produced while at

more positive potential (and for n-type Si at "high" light intensity) soluble oxides are formed and the semiconductor is electropolished [8].

There is a growing need for more robust (opto)electronic devices, capable of operating under extreme conditions. Wide-bandgap, chemically stable semiconductors can meet such a need [9]. The group IV compound semiconductor SiC is finding application in high-power transistors [10], sensors resistant to high temperature and caustic environment [11] and MEMS devices profiting from the mechanical and chemical properties of the semiconductor[12, 13]. With such developments there is a renewed interest in the wet chemistry and etching of SiC.

The electrochemistry of SiC in aqueous solution has not been nearly as well-studied as that of Si. Following the interest in porous Si in the early nineties, Shor and co workers showed that SiC can also be made porous by anodic etching in HF solution [14]. The p-type semiconductor dissolves in the dark, while supra-bandgap illumination is required to oxidize the n-type material. Like Si, n-type SiC can be made porous at strongly positive potentials in the dark (breakdown conditions) [15]. Okojie and co workers exploited the differences in anodic electrochemistry of n-type and p-type SiC to fabricate membranes for MEMS applications [16]. A recent study of n-type SiC in alkaline solution also showed similarities with the electrochemistry of Si [17]. In this paper we report further on both p-type and n-type SiC in alkaline solution and compare the results with those obtained for Si. We also describe results on SiC in acidic fluoride solution. For both systems we point out possible uses of (photo)anodic etching for practical device applications.

Experimental

Single crystal 6H-SiC (n-type) and 4H-SiC wafers (n- and p-type) (0001) were obtained from Cree (United States) and Umicore (Belgium). The n-type wafers were oriented on-axis, nitrogen-doped and had a resistivity of 0.01-0.07 Ω.cm. The p-type wafer (Cree) was oriented 8° off-axis, aluminium doped and had a resistivity of 3.86 Ω.cm. All samples used in this study had a Si polar face. For the electrochemical experiments, a circular opening was defined on the samples using a Si_3N_4 mask. The diameter of the opening was 2 mm. Ohmic contacts to the p-type SiC were made by evaporating a 300 nm thick layer of Al/Ta/Au on the back side of the wafer. The metallized wafer was

subsequently annealed at 850 °C for 10 minutes. The n-type wafers were contacted using a 300 nm Ti/Au layer followed by a 1 second annealing step at 1000 °C. The samples were mounted as a rotating disk electrode (RDE).

Czochralski-grown 4" (100) oriented Si wafers were obtained from Okmetic (Finland). The n-type wafers were phosphorus doped and had a resistivity of 1-10 Ω.cm. The resistivity of the p-type boron doped wafers was 5-10 Ω.cm. Ohmic contacts were provided on the backside using a GaIn eutectic. The Si samples (2x2 cm) were mounted in a Kel-F holder by means of a Viton O-ring.

Electrochemical measurements were performed in a three-electrode cell with a platinum counter electrode and a saturated calomel electrode (SCE) as a reference. A potentiostat (EG&G Princeton Applied Research, PAR-273-A) computer-controlled by LabVIEW was used to measure the current-potential curves in the dark and under illumination. The curves were recorded at a constant scan rate of 10 mV/s from negative to positive potential and back. The light source used for the electrochemical experiments was a Hg arc-lamp (500 W) with a power supply (Oriel 66941). UV light from the beam was directed on the sample using a dichroic mirror (280-400 nm). In order to increase the light intensity a plano convex lens was used to focus the beam on the electrode. In order to prevent heating of the substrate, a heat sink was used. The light intensity was varied with neutral density filters. Before the measurement, the samples were rinsed with acetone.

The etch rate was determined by measuring the etch depth with a surface profiler (Alpha-Step 500) and the surface morphology after etching was examined using a differential interference contrast (DIC) optical microscope (Nicon ECLYPSE ME 600), an atomic force microscope (Digital Instruments Nanoscope IIIa) and a scanning electron microscope (SEM JEOL 6330).

For the electroluminescence experiments a 0.1 M $K_2S_2O_8$, 0.5 M H_2SO_4 solution was used. The spectra were recorded with a CCD camera (Acton Research Corporation, Spectra Pro-300i).

Results and Discussion

High pH

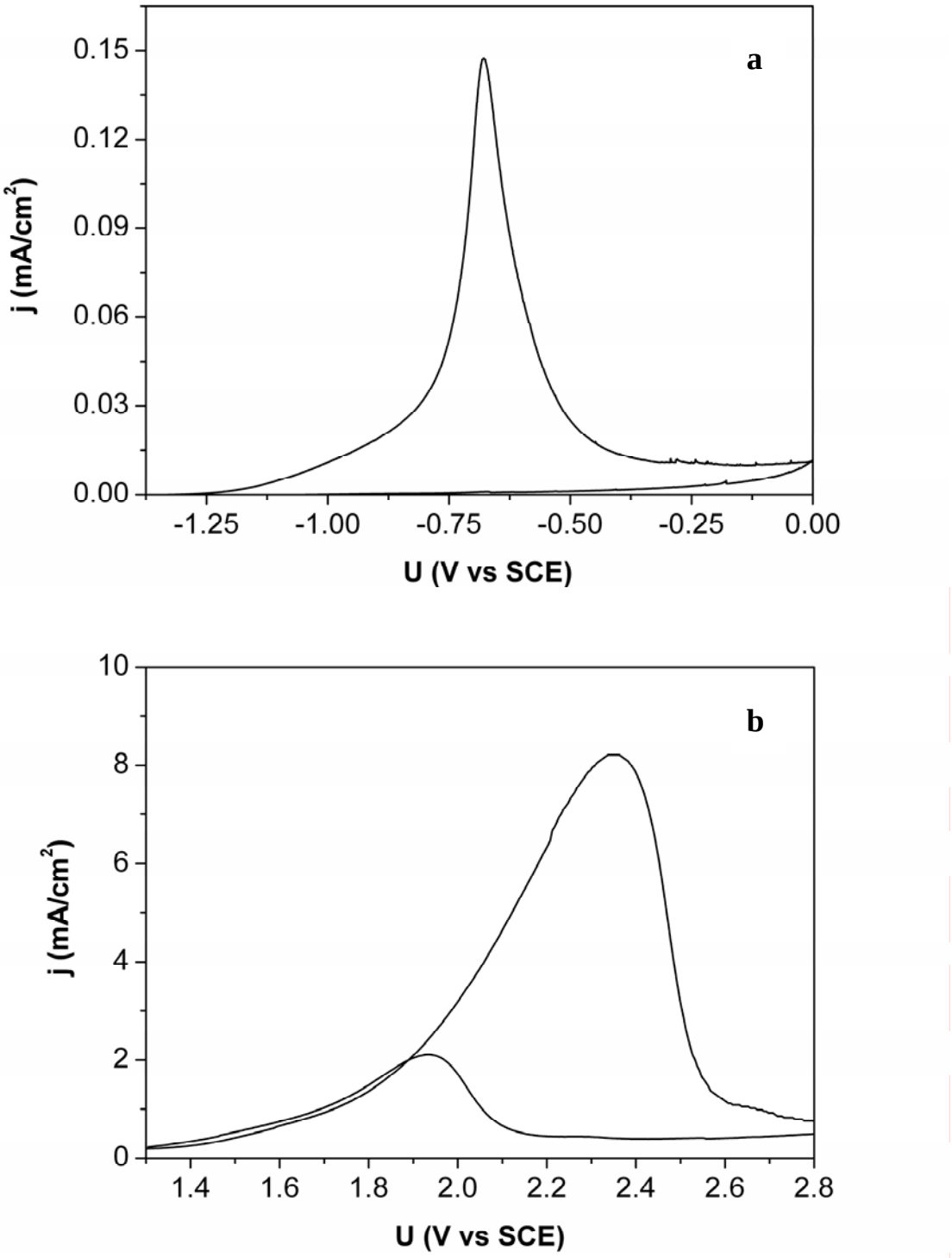

Figure 1. Current density-potential plots recorded for p-type Si and p-type 4H SiC (b) in 0.1M KOH solution at 20.5 °C. Both experiments were performed in the dark.

Figure 1(a) shows a typical current density-potential plot (j-U) for a p-type Si electrode in a 0.1 M KOH solution. No cathodic current is observed at negative potential: reduction of water to hydrogen requires conduction band electrons. As the potential is scanned to more positive values, a rapidly increasing anodic current is observed and the electrode finally passivates. Because of the presence of oxide on the surface, the current in the return scan is very low (the time required for chemical dissolution of the oxide is long). The j-U curve for p-type SiC in 0.1 M KOH solution (fig. 1(b)) shows features similar to those of p-type Si: an anodic current increasing as the potential is scanned to positive values, followed by passivation. There are two striking differences between the two semiconductors:

(i) - The onset of anodic current for SiC (1.4V) is much more positive than that for Si (-1.2V). This is due to the more positive flat-band potential of the wide-bandgap semiconductor [15]. The valence-band edge of SiC is at much lower energy than that of Si; consequently, hole injection into SiC from oxidizing agents in solution (essential for electroless etching) is not possible;

(ii) - The current density required for the passivation of SiC is a factor of 56 larger than that for Si at the same potential scan rate. This is very likely due to the presence of C in the compound semiconductor lattice, making it more difficult to form a protecting oxide.

As in the case of Si, the anodic current for SiC does not depend on the electrode rotation rate. In both cases the anodic current depends strongly on the OH^- ion concentration. This is shown for p-type SiC in fig. 2(a); the dependence of the anodic peak current density on OH^- ion concentration is given in fig. 2(b). From fig. 2(a) it is clear that the hysteresis in the voltammograms due to the passivation is reduced as the pH is increased; this is due to an increased oxide etch rate. From a comparison of the two semiconductors we conclude that the dissolution rate of the anodic oxide on SiC is considerably higher than that of the oxide on Si at the same pH (the hysteresis for Si in fig. 1a is more pronounced than that for SiC in fig. 1b). The peak current densities observed, correspond to etch rates ranging from 105 up to 523nm/min for a concentration span of 0.1-1.0 M of KOH (see right axis fig. 2(b)). The "activation energy" calculated from the temperature dependence of the peak current density for SiC (46 kJ/mol) indicates that the anodic reaction is kinetically controlled; this is in agreement with the lack of influence of rotation rate on the current.

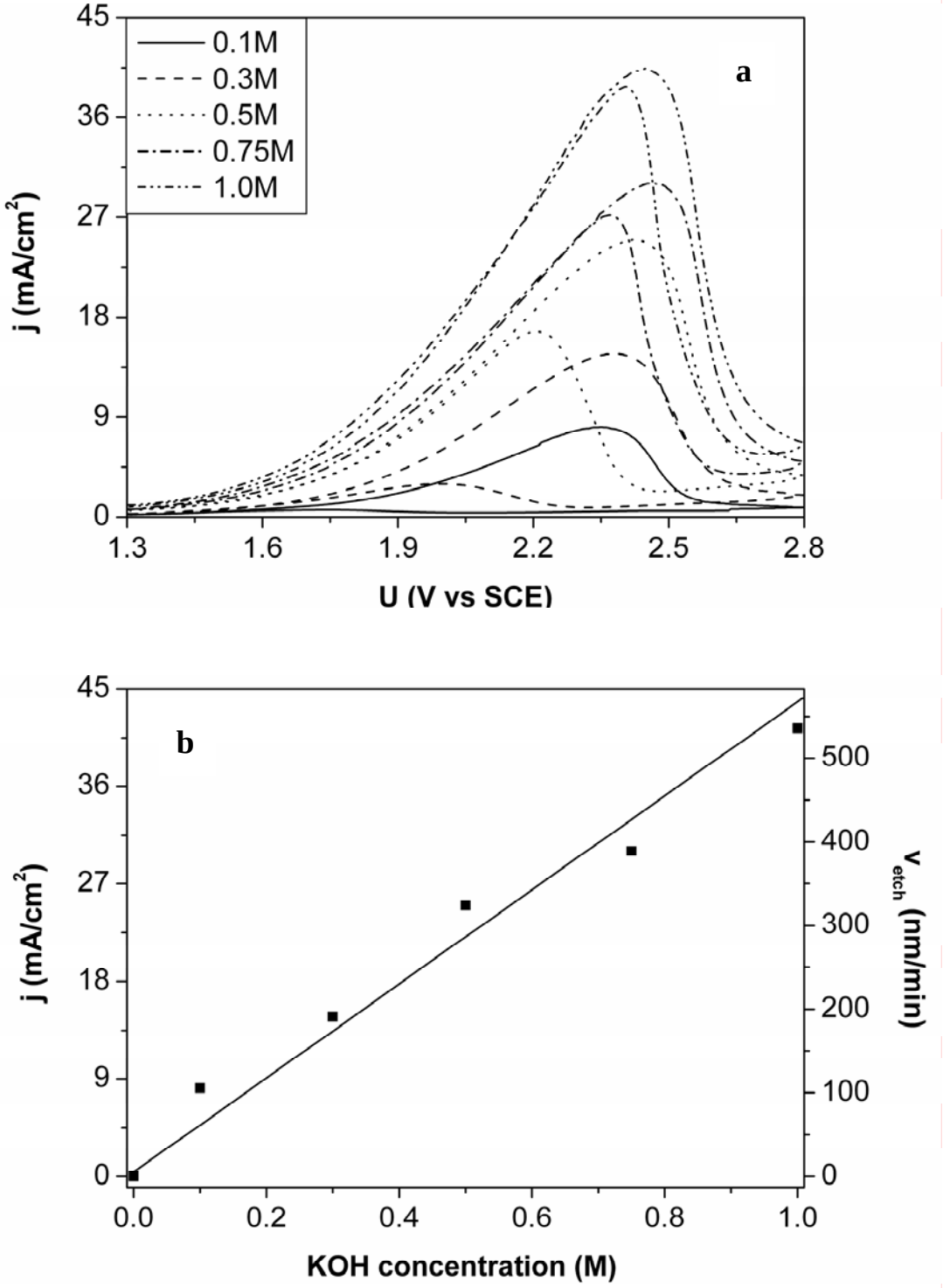

Figure 2. Current-potential curves for p-type 4H-SiC at different KOH concentrations at 20.5 °C (a). The values of the peak current and the passivation current are plotted against the KOH concentration (b). The rights axis shows the calculated etch rate.

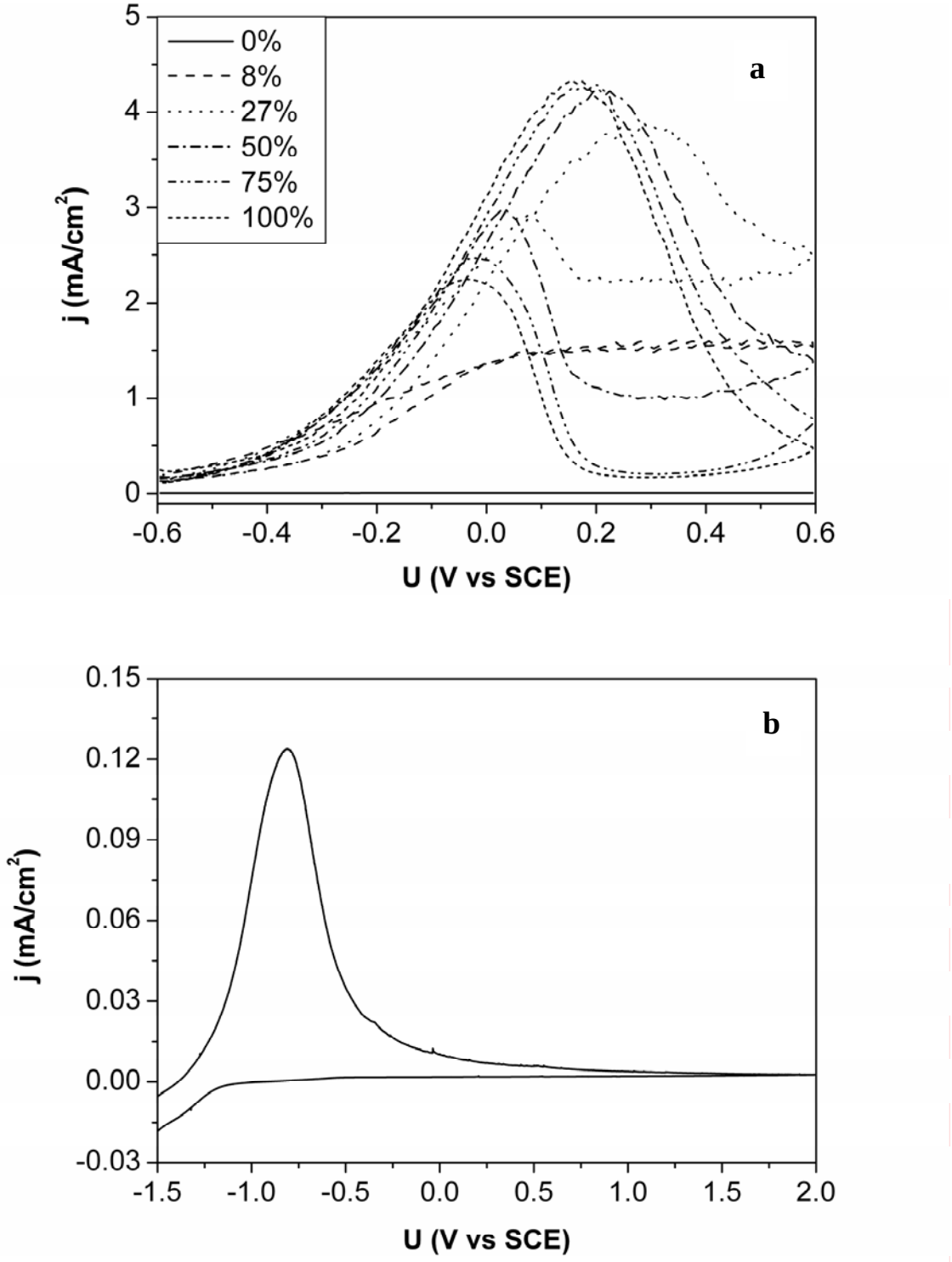

Figure 3. Current density-potential plots recorded for n-type 4H SiC at different light intensities (a) and n-type Si in the dark (b) in 0.1M KOH solution at 20.5 °C.

As one expects, n-type SiC is not anodically oxidized in the dark (fig. 3(a)). Hydrogen evolution gives rise to a cathodic current at negative potential. Under supra-bandgap illumination, anodic photocurrent is observed. At lower light intensity the limiting value is linearly dependent on the photon flux (this is not shown in fig. 3 (a)). At high photon flux the n-type electrode passivates at a current density similar to that required to passivate p-type SiC. Contrary to what we previously reported [18] the peak current density does not increase at higher light intensity [19]. In contrast to SiC, n-type Si can be anodically oxidized in the dark, giving rise to unexpectedly high current densities (fig. 3(b)); the current required to passivate p- and n-type Si at a given pH is almost the same (compare figures 1(a) and 3(b). The anodic reaction at n-type Si can be explained on the basis of the chemical etching, which occurs in alkaline solution at the oxide-free surface. Intermediates from this reaction give rise to states in the bandgap, from which electrons can be injected into the conduction band; this process gives an anodic current leading to oxidation and passivation of the electrode [5]. SiC does not etch chemically in aqueous solutions under these conditions.

The dissolution valency for SiC was determined by measuring simultaneously anodic charge and etch depth at various potentials between current onset and the peak. It was found that between 6 and 7 charge carriers are required to dissolve one formula unit of SiC. A valency of 6 indicates a reaction in which Si is oxidized to Si(IV) as silicate species in solution and the C forms CO:

$$SiC + 8OH^- + 6h^+(VB) \rightarrow [Si(OH)_2O_2]^{2-} + CO + 3H_2O \qquad [1]$$

Equation 1 allows us to convert current density to etch rate (see right axis, Fig. 2 (b)). Some CO_2 may also be formed accounting for the higher valency. The reaction in the passive range is, very likely, of the form:

$$SiC + 6OH^- + 6h^+ \rightarrow SiO_2 + CO + 3H_2O \qquad [2]$$

The RMS roughness of surfaces etched under these conditions was in the order of 20 nm. This is clearly not the finish required for a polished surface. However, the high etch rates that can be achieved anodically in KOH solution can be useful for removing damaged surface layers caused by wafer polishing. To follow the effects of photoanodic

etching of n-type SiC, we measured the electroluminescence of SiC in acidic solution. A strong oxidizing agent, the peroxydisulphate anion ($S_2O_8^{2-}$), was reduced at negative potential. This is a two-step reaction: the first is a conduction-band (CB) step producing the radical anion $SO_4^{-\cdot}$; this very strong oxidizing species can subsequently inject a hole into the valence band (VB):

$$S_2O_8^{2-} + e^- (CB) \rightarrow SO_4^{-\cdot} + SO_4^{2-} \quad [3]$$

$$SO_4^{-\cdot} \rightarrow SO_4^{2-} + h^+ (VB) \quad [4]$$

Electron-hole recombination can give light emission [20]. For the as-received sample a broad emission is found in the visible spectral range (curve (a) fig. (4)); this is very likely due to defect emission (donor-acceptor type). After removal of 10.3 μm of material by etching, the spectrum changed quite drastically (curve (b) fig. (4)). The intensity of the broad defect emission decreased and a sharp band with an energy just below the bandgap appeared. This is a clear indication of a favourable change in surface properties due to etching.

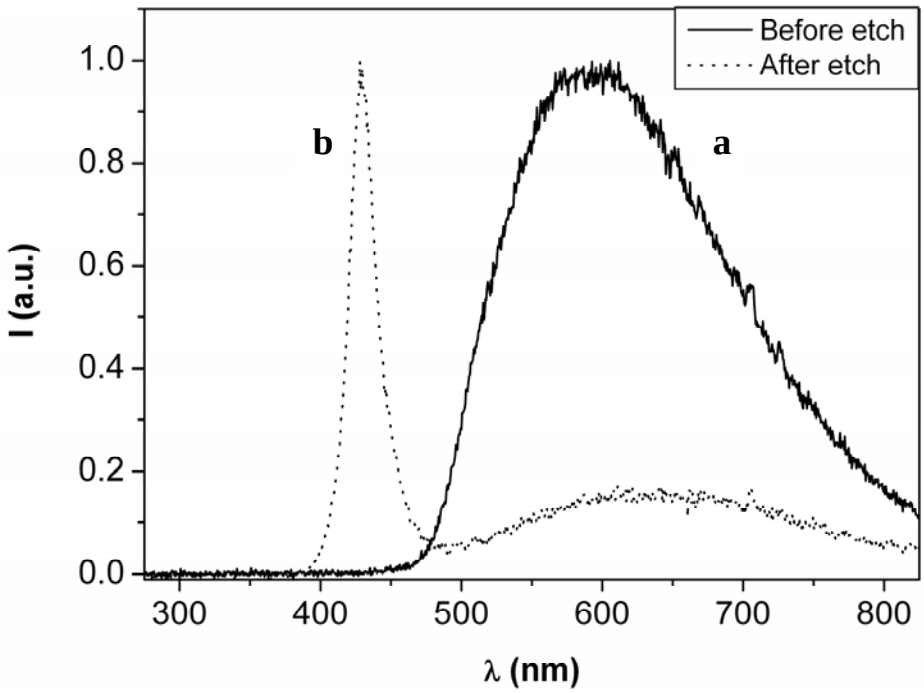

Figure 4. Electroluminescence spectra of n-type 6H SiC as received (straight line) and after removal of a 10.3 μm thick crystal layer (dotted line).

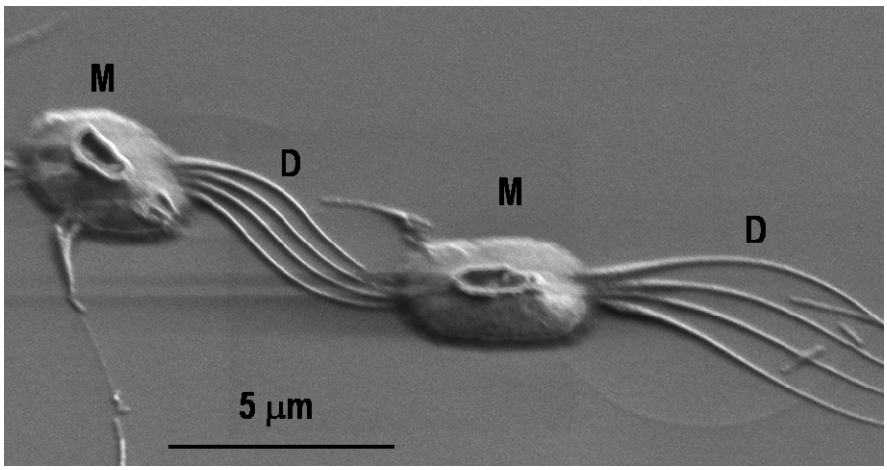

Figure 5. SEM image of etch features formed on micropipes (M) and pinning dislocations (D) parallel to the (0001) Si surface of a SiC substrate revealed by defect selective photoanodic etching.

Photoanodic etching of n-type SiC can be used not only for removing damage but also for revealing defects. In the lower part of the photocurrent-potential curve, electron-hole recombination competes with the hole reaction (oxidation of the solid). Since crystallographic imperfections act as very effective recombination centers, etching at such defects is (partly) suppressed, giving rise to hillocks (see fig. 5).

The fact that only Si can be etched chemically and that there are considerable differences in the electrochemistry of Si and SiC, offers a number of options for material-selective etching, interesting for MEMS. These include selective etching of either p-type or n-type SiC in a p-n junction, and selective etching of SiC with respect to Si or *vice versa* [17].

Low pH

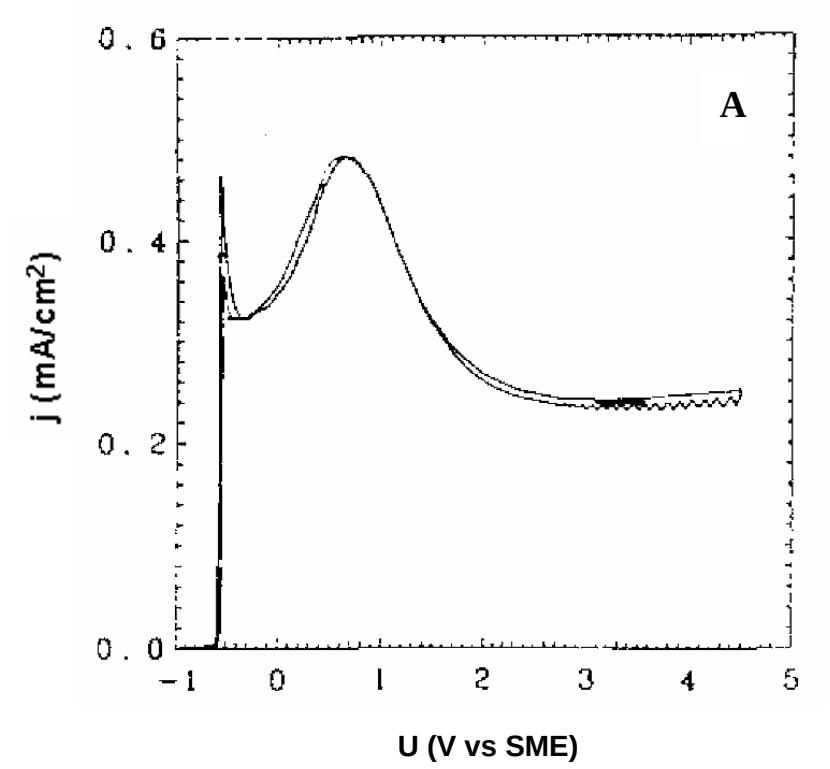

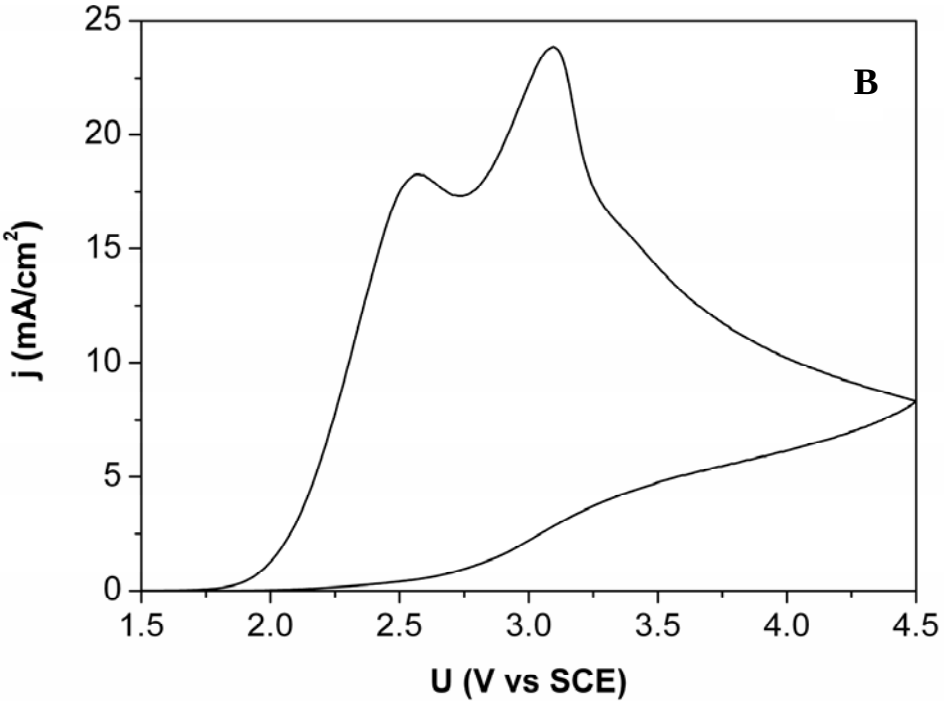

Figure 6. Current density-potential plots recorded in fluoride media (c_f = 33mM, pH=3) for p-type Si [21](a) and p-type 4H SiC (b). The rotation rates used were 1600 RPM and 1500 RPM for Si and SiC respectively. Note: In fig 6(a) the potential is given with respect to a saturated mercury/mercurous sulfate (SME) reference electrode.

For anodic oxidation of Si in fluoride solution at low pH, valence band holes are essential: p-type Si dissolves in the dark, while illumination is required for the n-type electrode [21-23]. Fig. 6(a) shows results of Hassan *et al.* for p-type Si at pH 3. In the current onset porous Si is formed. At more positive potentials, oxide formation gives rise to a number of peaks in the voltammogram (the nature of the oxide depends on the potential). Measurements in this range at different rotation rates showed the anodic reaction to be under mixed transport-kinetic control. In the reverse scan current oscillations and some hysteresis are observed. The current-potential characteristics of p-type SiC (fig. 6(b)) show features similar to those of p-type Si. The peaks in the voltammogram suggest the formation of soluble oxides.

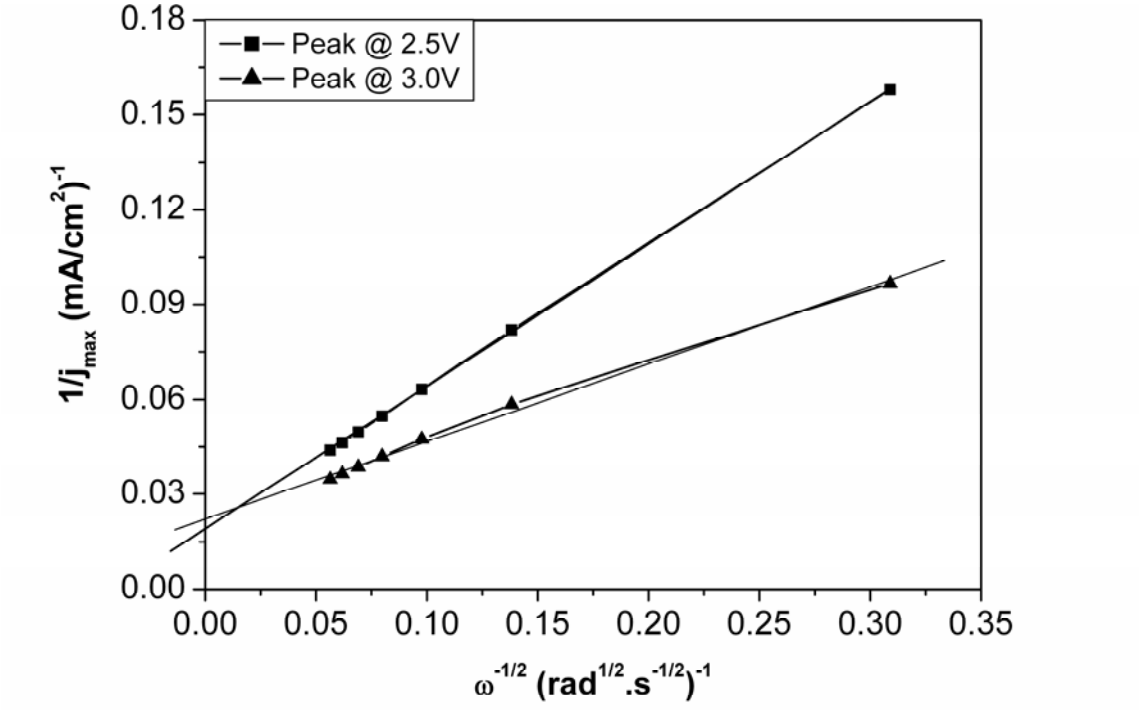

Figure 7. Koutecky-Levich plot based on the measurements performed in a 33 mM fluoride solution. The rotation rates were varied between 100-3000 RPM.

Fig. 7 shows a Koutecky-Levich analysis [21] of the first and second peaks in the voltammogram: the inverse of the peak current is plotted as a function of the inverse of the square root of the rotation rate. The straight lines with intercept on the y-axis show that, as in the Si case, anodic oxidation is under mixed transport-kinetic control. For both semiconductors the form of the voltammogram depends on the composition of the solution. Two differences observed at high pH values are also found in fluoride solution: current onset for p-type SiC is at a markedly more positive potential than for p-type Si (due to the difference in flat-band potential) and the current required for oxide formation (the first peak) is much higher in the case of SiC. Curiously, a much stronger hysteresis is observed in the SiC case, suggesting the presence of a more resistive oxide. This is the opposite to what we observe in alkaline solution (fig. 1(b)). In contrast to anodic etching of SiC at high pH, a much better surface finish can be obtained in the acidic fluoride solutions (an RMS roughness of 5 nm). This is perhaps not surprising since it is known that Si is electropolished under these conditions [24].

Conclusions

Like Si, both p-type and n-type SiC undergo anodic oxidation and passivation in KOH solution. The current-potential characteristics of p-type SiC resemble those of p-type Si, but much higher current densities are required for passivation of the compound semiconductor. Unlike Si, n-type SiC is anodically oxidized and passivated only under supra-bandgap illumination. In acidic fluoride solution both p-type semiconductors show anodic oxidation and, at more positive potentials, non-passivating oxide formation. On the basis of this study we discuss dissolution mechanisms of SiC in aqueous solution. In addition, we point out a number of applications interesting for SiC device technology. Furthermore, the electroluminescence of SiC in acidic peroxydisulphate solution was observed and the effect of photoanodic etching on this process is shown.

Acknowledgements

The authors would like to thank Ruud Balkenende (Philips Research, The Netherlands), Hans Ligthart and Harold Philipsen for contributing to this work. This work was financially supported by the Dutch Technology Foundation (STW, UPC-6317).

References

[*1*] Seidel H, Csepregi L, Heuberger A, and Baumgartel H, *J. Electrochem. Soc.* 137 (1990) 3612.

[*2*] Vellekoop M J, Vanrhijn A J, Lubking G W, and Venema A, *Sensors and Actuators a-Physical* 27 (1991) 699.

[*3*] Tirole N, Hauden D, Blind P, Froelicher M, and Gaudriot L, *Sensors and Actuators a-Physical* 48 (1995) 145.

[*4*] Faust J W, Jr.; Palik, E D, *J. Electrochem. Soc.* 130 (1983) 1413.

[*5*] Xia X H, Ashruf C M A, French P J, Rappich J, and Kelly J J, *J. Phys. Chem. B* 105 (2001) 5722.

[*6*] Ashruf C M A, French P J, Bressers P, Sarro P M, and Kelly J J, *Sensors and Actuators a-Physical* 66 (1998) 284.

[*7*] Collins S D, *J. Electrochem. Soc.* 144 (1997) 2242.

[*8*] Lehmann V, Electrochemistry of Silicon, WILEY-VCH Verlga GmbH, Weinheim, 2002.

[*9*] Wang S W, Di Ventra M, Kim S G, and Pantelides S T, *Phys. Rev. Lett.* 86 (2001) 5946.

[*10*] Di Ventra M and Pantelides S T, *Phys. Rev. Lett.* 85 (2000) 1782.

[*11*] Willander M, Friesel M, Wahab Q U, and Straumal B, *Journal of Materials Science-Materials in Electronics* 17 (2006) 1.

[*12*] Connolly E J, Timmer B, Pham H T M, Groeneweg J, Sarro P M, Olthuis W, and French P J, *Sensors and Actuators B-Chemical* 109 (2005) 44.

[*13*] Sarro P M, *Sensors and Actuators a-Physical* 82 (2000) 210.

[*14*] Shor J S, Grimberg I, Weiss B Z, and Kurtz A D, *Appl. Phys. Lett.* 62 (1993) 2836.

[*15*] van de Lagemaat J, Vanmaekelbergh D, and Kelly J J, *J. Appl. Phys.* 83 (1998) 6089.

[*16*] Okojie R S, Ned A A, and Kurtz A D, *Sensors and Actuators a-Physical* 66 (1998) 200.

[*17*] vanDorp D H K, J J; Weyher J L, *Journal of Micromechanics and Microengineering* in Press (2007) xxx.

[*18*] vanDorp D H and Kelly J J, *J. Electroanal. Chem.* 599 (2007) 260.

[*19*] p. The increase in peak current with increasing light intensity reported in ref. [18] was due to a thermal effect.

[*20*] Kelly J J, Kooij E S, and Meulenkamp E A, *Electrochim. Acta* 45 (1999) 561.

[*21*] Hassan H H, Sculfort J L, Etman M, Ozanam F, and Chazalviel J N, *J. Electroanal. Chem.* 380 (1995) 55.

[*22*] Etman M, Neumannspallart M, Chazalviel J N, and Ozanam F, *J. Electroanal. Chem.* 301 (1991) 259.

[*23*] Chazalviel J N, Etman M, and Ozanam F, *J. Electroanal. Chem.* 297 (1991) 533.

[*24*] Zhang X G, Collins S D, and Smith R L, *Journal of the Electrochemical Society* 136 (1989) 1561.